Influence of Yb-Doped Nanoporous TiO_2 Films on Photovoltaic Performance of Dye-Sensitized Solar Cells *

XU Wei-Wei(徐炜炜), DAI Song-Yuan(戴松元)**, HU Lin-Hua(胡林华), LIANG Lin-Yun(梁林云), WANG Kong-Jia(王孔嘉)

Institute of Plasma Physics, Chinese Academy of Sciences, Hefei 230031

(Received 25 April 2006)

Yb-doped TiO_2 pastes with different Yb/TiO_2 weight ratios are prepared in the sol-gel process to obtain dye-sensitized solar cells (DSCs). The nanocrystalline size of Yb-TiO_2 becomes smaller and the lattice parameters change. Lattice distortion is observed and dark current is detected. It is found that a part of Yb existing as insulating oxide Yb_2O_3 state acts as barrier layers at the electrode–electrolyte interface to suppress charge recombination. A Yb-doped TiO_2 electrode applied in DSCs leads to a higher open-circuit voltage and a higher fill factor. How the Yb-doped TiO_2 films affect the photovoltaic response of DSCs is discussed.

PACS: 84. 60. Jt, 68. 55. Jk, 68. 55. Ln

Dye-sensitized solar cells (DSCs) have been intensively studied for their simple assembly technology and their potential low cost.[1−3] Nanoporous crystalline TiO_2 film electrodes are a crucial component of DSCs. In research of photoanode materials, although dye-sensitization has been achieved with high band gap semiconductor porous films of non-TiO_2 materials such as SnO_2,[4] Fe_2O_3,[5] Al_2O_3,[6], ZnO,[7] it has never been reported to be as efficient as that based on TiO_2.

Recently, a new record of photoelectric conversion efficiency up to 11.04% in full AM 1.5 sunlight was achieved by the EPFL group.[8] The nanoporous semiconductor electrode, as one of the more puzzling components of DSCs, receives various studies for a better understanding of its operation and better energy conversion efficiency.[9,10] Since the difference between the electron Fermi level in TiO_2 and the redox potential of the electrolyte, which corresponds to V_{oc}, one possible way for increasing V_{oc} is to enhance the negative value of the conduction band of the material used in electrodes.[11] Moreover, the charge recombination between the electrons injected in the conduction band of semiconductors and the oxidized species in the electrolyte still remains one of the major limiting factors to improve the efficiency of DSCs. It has recently been suggested that coating a blocking overlayer on the surface of such a nanoporous film may be an important approach to retard the charge recombination and to improve the performance of DSCs.[12−16]

Some researchers reported that lanthanide ions doped in TiO_2 nanoparticles could suppress the recombination of electron–hole pairs and prolong the lifetime of carriers, which is essential for improving the efficiency of both the net charge transfer at the semiconductor/electrolyte interface and the separation efficiency of carriers.[17,18] Therefore, introducing the lanthanide ion ytterbium (Yb) into the TiO_2 nanocrystalline films should modulate the performance of DSCs.

In this Letter, we report how the Yb-doped TiO_2 nanocrystalline material is prepared and characterized with several measurements. The microstructure of the Yb-doped TiO_2 films is discussed in detail, focusing on the ability of such lanthanide ions influencing the electron injection and charge recombination among the DSCs. The results confirm that Yb plays an important part in modulating the electron transport, especially in back reaction, consequently enhances the open-circuit voltage V_{oc} and the fill factor (FF).

Titanium isopropoxide (100 mL, Fluka) was added dropwise to 180 mL deionized water to form a white precipitate under vigorous stirring. A quantity of triethylamine was added to adjust the pH value to 11. Then stirred vigorously for 8 h at 80°C to form a transparent TiO_2 sol and heated at 250°C in autoclave for 15 h to obtain TiO_2 gelatin. After that, the water in gelatin was removed by a rotary evaporator. $YbCl_3$ solution in anhydrous ethanol with different concentrations and surfactants were added and dispersed in the gelatin. Finally, the colloidal pastes with different weight ratios of Yb/TiO_2 were obtained by evaporating the ethanol at room temperature.

The TiO_2 and Yb-TiO_2 pastes were applied onto TCO glass (TEC-8, LOF) using the screen-printing technique. The resulting films were dried and sintered to form 16-μm-thick doped/undoped TiO_2 photoanodes. Coating the TiO_2 film surface with dye was carried out by soaking the film in a 5.0×10^{-4} mol/L solution of bis(tetrabutylammonium) cis-dithiocyanatobis(2,2′-bipyridine-4-COOH,4′-COO^-) ruthenium(II) (N719) in anhydrous ethanol.

Thermally platinized TCO was used as

* Supported by the National Key Basic Research Special Foundation of China under Grant No G2000028206.
** To whom correspondence should be addressed. Email: sydai@ipp.ac.cn
©2006 Chinese Physical Society and IOP Publishing Ltd

the counter electrode, which was printed using a paste based on H_2PtCl_6. The electrolyte containing 0.6 mol/L DMPII (1,2-dimethyl-3-propyl imidazolium), 0.1 mol/L LiI, 0.1 mol/L I_2, 0.5 mol/L TBP (tert-butylpyridine) and MePN (3-Methoxypropionitrile) was capillary injected through prearranged small ports at the counter-electrode, which was then sealed with hot melt.

The film thickness was determined with a surface profilometer (Ambios Technology XP-2). X-ray diffraction (XRD) was carried out in a D/Max-rB powder x-ray diffractometer by using Cu K_α radiation (at 40 kV, 100 mA). High-resolution transmission electron micrographs (HRTEM) were recorded on an electron microscope of JEM-2010 at 200 kV. The particle size of TiO_2 and Yb-TiO_2 powder and the electrode microstructure were studied using a field emission scanning electron microscopy (FE-SEM, Sirion 200, FEI corp). Linear sweep voltammeter (LSV) curves of DSCs were performed to obtain the dark current with an electrochemical workstation (CHI660A, CH Instruments, Inc. USA). The current–voltage (I–V) characteristics of the DSCs (I_{sc}, V_{oc}, FF and η) were derived with a Keithley 2420 source meter controlled by Testpoint software under a xenon lamp (AM1.5), calibrated by a standard crystalline silicon solar cell and pyrometer. The effective area for illumination was 0.16 cm^2.

Table 1. Crystallite size D_{hkl} and lattice distortion of Yb-doped and undoped TiO_2.

M_{Yb}/M_{TiO_2} (wt.%)	D_{hkl} (nm)	$a=b$ (Å)	c (Å)	a/c	δ (a/c) (%)
undoped	18.3	3.81092	9.51624	0.40046	–
0.06	16.1	3.78020	9.49416	0.39816	−0.23
1.5	17.1	3.77372	9.48624	0.39781	−0.27
6	18.2	3.77368	9.51732	0.39651	−0.40

Figure 1 shows the x-ray diffraction patterns of the samples. The XRD spectra imply that the dopant has no obvious effect on the formation of TiO_2 phase. Yb–TiO_2 powder is still in pure anatase phase, where separate Yb_2O_3 phase or other phases have not been detected. The average crystallite size D_{hkl} of the powders is calculated from the Scherrer equation $D_{hkl} = K\lambda/\beta\cos\theta$. From Table 1, the D_{hkl} of Yb-doped TiO_2 is smaller than that of the undoped one. In our opinion, the decrease of D_{hkl} is due to the suppression to the crystallite growth of TiO_2 particles by the lanthanide ion doping. Figure 2 shows the enlarged XRD patterns around the peak of crystal plane (101) of pure TiO_2 and the binary oxide samples. Since the ionic radius of Yb (0.860 Å) is larger than that of Ti (0.605 Å),[19] the (101) diffraction peak of the anatase type titania shifts gradually to a lower 2θ angle with the increasing Yb content, which suggests that Yb may substitute Ti or possibly occupy the hole in anatase cell. This result is analogous to that reported by Yu *et al.*[20] The peaks of the samples that contain less Yb almost have no shift, which probably means that Yb may present as Yb_2O_3. Because the XRD peaks from Yb_2O_3 cannot be observed even when the Yb content is 6 wt.%, it may be attributed to the Yb_2O_3 amorphous phase or the small amount.

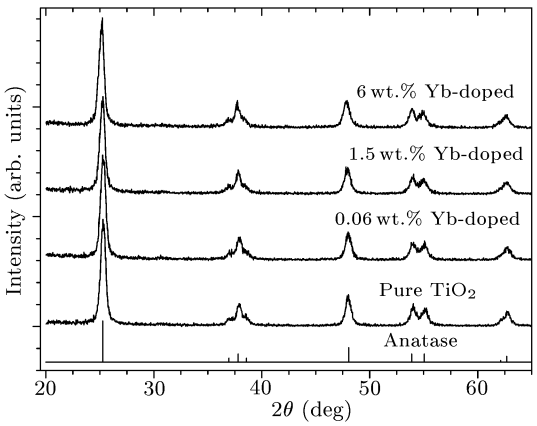


Fig. 1. X-ray diffraction patterns of samples.

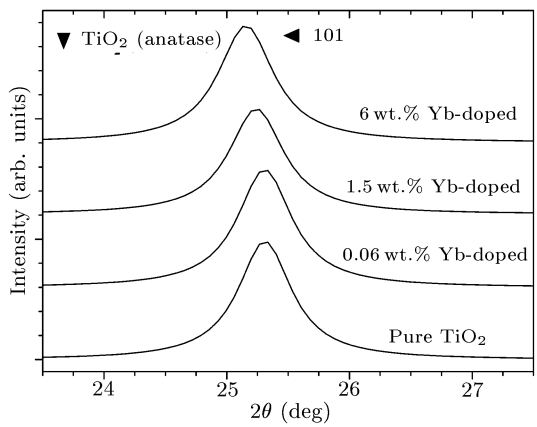


Fig. 2. X-ray diffraction peaks of crystal plane (101).

The peaks of crystal planes (101) and (004) in anatase are selected to determine the lattice parameters of the Yb-doped and undoped TiO_2 samples. The lattice parameters are calculated by the equations

$$D(hkl) = \lambda/2\sin\theta, \quad \text{Bragg's law},$$
$$D^{-2}(hkl) = h^2a^{-2} + k^2b^{-2} + l^2c^{-2},$$

where hkl is the crystal plane index; a, b, and c are the lattice parameters (in anatase phase, $a = b \neq c$); $D(hkl)$ is the distance between crystal planes of (hkl); λ is the x-ray wavelength; θ is the diffraction angle of the crystal planes (hkl). In Table 1, $\delta(a/c)$ represents the lattice distortion of Yb-doped sample. Here $\delta(a/c) = a/c - a_0/c_0$, a/c and a_0/c_0 denotes the ratios between the lattice parameters of doped and undoped TiO_2. It is obvious that with the increasing dopant concentration, the lattice distortion is boosted up accordingly.

Furthermore, the dislocation feature is shown in

Fig. 3 by HRTEM, which confirms the existence of lattice distortion brought by Yb. The distortion shift of the crystal plane (103) stripe is up to 0.162 nm. Thus surface states or trap states may exist in Yb-doped TiO_2, which would influence the crystal lattice and increase the probability of electrons trapping.

The surface structures of the powder and the film samples are indicated in Fig. 4. The observation of FE-SEM shows that the morphology of Yb-doped TiO_2 powder (Fig. 4(b)) is similar to that of undoped one (Fig. 4(a)) prepared in the same condition. And lanthanide ion Yb affects the growth of particles, so the aggregation happens, but it is hard to distinguish the Yb_2O_3 and Yb-TiO_2 particles from the surface microcosmic morphology.

Typical data obtained under AM1.5 simulated solar irradiance is listed in Table 2. It is apparent that V_{oc} shifts to the higher value with the concentration of Yb increasing. The maximal V_{oc} is found to be 0.75 V for the cell based on the 6 wt.% Yb-doped TiO_2 electrode, increasing by 8.7% relative to 0.69 V for the undoped film electrode. Furthermore, the FF also increases by 9.5% according to that of the undoped one. While the short-circuit photocurrent density J_{sc} and the overall light to electricity conversion efficiency η decrease with the increasing concentration of Yb.

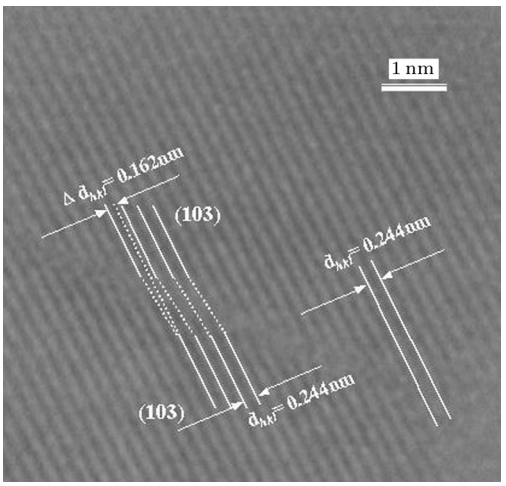


Fig. 3. HRTEM micrographs demonstrating the dislocation feature of the Yb-doped TiO_2 crystal lattice.

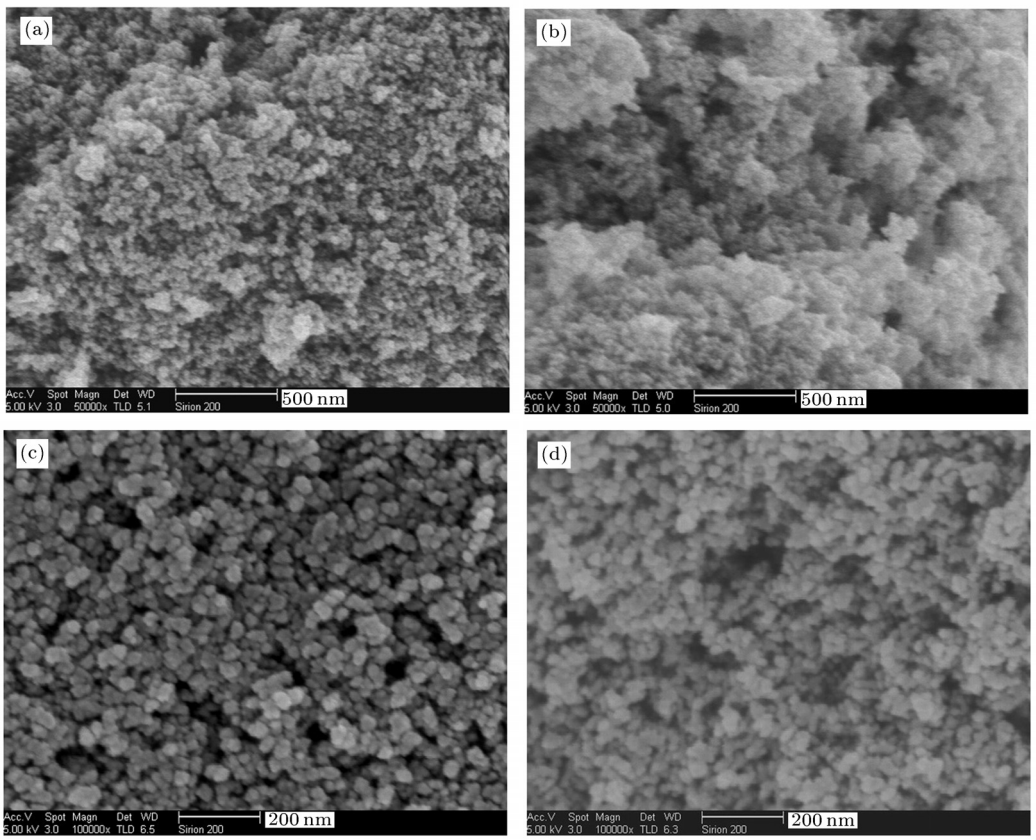


Fig. 4. FE-SEM images of (a) undoped TiO_2 powder, (b) Yb-doped TiO_2 powder, (c) undoped TiO_2 film electrode, (d) Yb-doped TiO_2 film electrode.

The dark current data can be observed in Fig. 5. When a positive potential is applied between the photoelectrode and the counter electrode, the electrons transfer under the electric field force and are trapped by different recombination pathways. Figure 5 illustrates that Yb-doped DSCs exhibit smaller dark current, which indicates that Yb treatment could successfully retard the charge recombination, similar to the results obtained by other improvement research.[16,18]

In DSCs, a widely accepted concept is that charge

Table 2. Influence of different treated concentrations on the performance of DSCs.

Treated concentration (wt.%)	V_{oc} (V)	J_{sc} (mA/cm^2)	FF (%)	η (%)
undoped	0.69	13.38	63	6.04
0.06%	0.71	11.64	67	5.55
1.5%	0.73	10.20	67	4.95
3%	0.74	8.77	69	4.36
6%	0.75	6.26	69	3.15

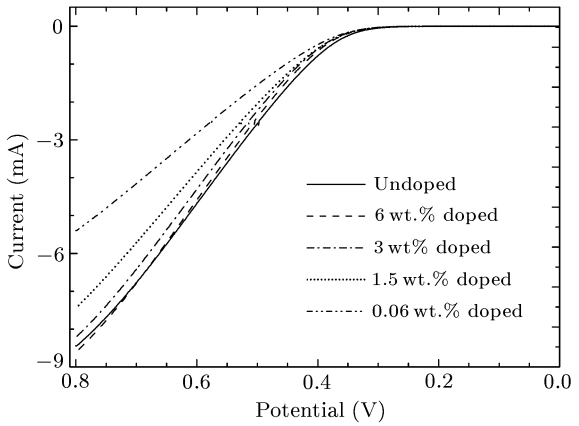


Fig. 5. Linear sweep voltammeter (LSV) curves of DSCs.

collection is largely limited by kinetic competition between charge transport in the TiO_2 film and/or electrolyte and interfacial charge recombination. When the cell operates under load, the kinetic competition is expected to be particularly critical owing to the highest electron density and the most critical recombination dynamics. In our experiment, this competition is investigated. It is suggested that Yb may enter into the lattice of TiO_2 or possibly occupy the hole in anatase cell, which result in the lattice distortion and the dislocation observed by XRD and HRTEM measurements. Thus some surface states may be brought and influence the electron transport. However, the actual doping concentration of lanthanide ion in TiO_2 is related to the ionic radii. Most of the ionic radii of lanthanide ions are much larger than that of Ti^{4+}, so lanthanide ions are difficult to enter into the lattice of TiO_2. According to Yb^{3+}, the content of Yb entering into the lattice of TiO_2 may be much lower. A amount of Yb_2O_3 exists to form an energy barrier at the electrode-electrolyte interface to retard the charge recombination. From Fig. 5, nearly all the DSCs fabricated with Yb-doped TiO_2 photoanodes have low back current, which implies that the Yb_2O_3 insulating layer plays a major role in the kinetic competition. We suggest that the back reactions of DSCs in the presence of the lattice defects take place by the mechanism

$$I_3^- + 2e_{cb}^-(TiO_2) \rightarrow 3I^-,$$
$$TiO_2(e_{cb}^-) + TiO_2(h^+) \rightarrow TiO_2$$

Because the retardation of interfacial recombination results from the Yb_2O_3 insulating oxide blocking layer, the electron density in the TiO_2 conduction band and the quasi-Fermi level of TiO_2 are heightened accordingly, and V_{oc} is higher than that of bare TiO_2-based DSCs. The increase of FF indicates that loss mechanisms such as recombination in semiconductor photoconversion have been minimized. Furthermore, the difference between the higher quasi-Fermi level and the LUMO of N719 dye is reduced, which results in the weakening driving force for the photoelectron injecting from the dye excited state into the conduction band of TiO_2. That is to say, the velocity of the electron injection process becomes slower. Yb_2O_3 existing among the pores of the TiO_2 film may also decrease the amount of dye sensitizer adsorption and may influence the diffusion and transport of the electrolyte. Therefore, J_{sc} becomes lower accordingly.

In conclusion, the influences of the lanthanide ion Yb on the TiO_2 crystal lattice and the performances of DSCs have been investigated. Yb-TiO_2 powder is still in pure anatase phase, in which no separate Yb_2O_3 phase and other phase have been detected. By calculating and comparing the lattice parameters, it can be concluded that large Yb content can result in lattice distortion and dislocation, which may bring on some trap states. A part of Yb presenting as am insulating barrier layer can retard the charge recombination. V_{oc} and FF increase by 8.7% and 9.5% separately though J_{sc} and η decline. More researches are underway in our group to investigate the advantage of DSC optimization in wider regions.

References

[1] O'Regan B and Grätzel M 1991 *Nature* **353** 737
[2] Nazeeruddin M K et al 1993 *J. Am. Chem. Soc.* **115** 6382
[3] Dai S Y and Wang K J 2003 *Chin. Phys. Lett.* **20** 953
[4] Dabestani R et al 1988 *J. Phys. Chem.* **92** 1872
[5] Fitzmaurice D J and Frei H 1991 *Langmuir* **7** 1129
[6] Nuesch F et al 1996 *J. Am. Chem. Soc.* **118** 5420
[7] Rensmo H et al 1997 *J. Phys. Chem.* B **101** 2598
[8] Grätzel M 2004 *J. Photoch. Photobiol. A: Chem.* **164** 3
[9] Wang Z S, Kawauchi H, Kashima T and Arakawa H 2004 *Coordinat. Chem. Rev.* **248** 1381
[10] Xu W W et al 2005 *Acta Phys. Sin.* **54** 5943 (in Chinese)
[11] Burnside S et al 1999 *J. Phys. Chem.* B **103** 9328
[12] Tennakone K, Kumara G R R A, Kottegoda I R M and Perera V P S 1999 *Chem. Commun.* **7** 15
[13] Kumara G R R A et al 2001 *J. Phys. D: Appl. Phys.* **34** 868
[14] Lenzmann F et al 2001 *J. Phys. Chem.* B **105** 6347
[15] Palomares E et al 2003 *J. Am. Chem. Soc.* **125** 475
[16] Wang P, Wang L D, Li B and Qiu Y 2005 *Chin. Phys. Lett.* **22** 2708
[17] Wang Y Q et al 2000 *J. Molecular Catalysis A: Chem.* **151** 205
[18] Yang S M, Li F Y and Huang C H 2003 *Sci. Chin.* B **33** 59 (in Chinese)
[19] Shannon R D 1976 *Acta Crystallogr.* A **32** 751
[20] Yu J C, Lin J and Kwok R M 1998 *J. Phys. Chem.* B **102** 5094